



Unveiling the Impact of Potential Evapotranspiration Method Selection on Trends in Hydrological Cycle Components Across Europe

Vishal Thakur¹, Yannis Markonis¹, Rohini Kumar², Johanna Ruth Thomson¹, Mijael Rodrigo Vargas Godoy^{1,3}, Martin Hanel¹, and Oldrich Rakovec^{1,2}

¹ Faculty of Environmental Sciences, Czech University of Life Sciences Prague, Kamýcká 129, Praha – Suchbátka, Czech Republic

³ River-Coastal Science & Engineering, Tulane University, New Orleans, 70118, Louisiana, USA

² Department Computational Hydrosystems, UFZ-Helmholtz Centre for Environmental Research, Leipzig, Germany

Correspondence: Vishal Thakur (thakur@fzp.czu.cz)

Abstract. Hydrological models are essential tools for assessing and predicting changes in the hydrological cycle, offering detailed quantification of components like runoff (Q), total water storage (TWS), and actual evapotranspiration (AET). Precipitation (PRE) and potential evapotranspiration (PET) are the major required drivers for modeling these components. In modeling, the linkage of PRE to changes in these cycle components is well understood compared to PET. Here, we focus on the changes in PET and their influence on hydrological cycle components (AET, Q, and TWS). We consider 12 distinct PET methods from three different categories (temperature-based, radiation-based, and combination type) across 553 European catchments. The mesoscale Hydrological Model (mHM) was used to simulate 40 years of hydrological components, with a total of 6 636 mHM runs. Comprehensive trend analysis and data concurrence index (DCI) based on trend direction were applied to three different catchment categories (energy-limited, water-limited and mixed depending on PET method) to assess changes in PET and its influence on AET, Q, and TWS. PET methods exhibit diverse annual and seasonal trends across catchment categories for PET, AET, Q, and TWS. While PET demonstrate strong agreement in trend directions, the trend magnitudes vary depending on the choice of PET method. The findings reveal that the Jensen-Haise method produces the highest trends for PET on both annual and seasonal scales (summer, spring, and autumn), whereas no single PET method consistently represents the lowest trend. AET trends are similar to those of PET but are lower in trend magnitude at annual scale, while seasonally, only energy-limited catchments show a trend pattern similar to PET. Across all PET methods, there is strong agreement in trend direction, except



during the winter season. For the majority of European catchments, Q and TWS show strong agreement among different methods, either positive or negative. In the annual trend, the summer season largely contributes to PET. For AET, summer season largely contributes to the annual trend only in energy-limited and water-limited catchments. Overall, studies focusing on the directional changes in the hydrological cycle or its components indicate that PET methods have a limited impact. However, when quantifying changes in hydrological cycle components, the choice of PET method becomes crucial. Therefore, selecting the appropriate PET method is crucial for studies on AET, Q, and TWS.



1 Introduction

In 1948, Thornthwaite (1948) introduced the concept of potential evapotranspiration (PET), which is the potential to evaporate water from the land surface to the atmosphere without any limitation to water availability. PET is used in diverse research fields. In agriculture, it is employed for irrigation scheduling and modeling crop water requirements (Xiang et al., 2020). In environmental studies, PET is used for aridification research and investigating extreme events, including meteorological, agricultural, and hydrological droughts (Park et al., 2018; Zhou et al., 2023; Shi et al., 2023a). In hydrology, it is used to determine the long-term states of catchments, such as energy-limited and water-limited catchments, and it plays a key role in the Budyko framework for estimating long-term changes in hydrological components (Reaver et al., 2022). Furthermore, PET is extensively used in hydrological modeling as to define the maximum rate of possible water loss through evaporation and transpiration. It is used as one of the important input variables to simulate key hydrological, such as actual evapotranspiration (AET), runoff (Q), and total water storage (TWS).

Since the Thornthwaite's study, more than 50 empirical PET equations have been developed, ranging from simple to complex types (Lu et al., 2005). They can be classified mainly into three categories based on input data: (1) Temperature-based methods, which utilize temperature as input (Shaw and Riha, 2011). Due to their simplicity and minimal data requirement, these are widely used in the hydrological model (Arnold et al., 1998; Liu et al., 2008). (2) Radiation-based methods require solar radiation (short wave or net radiation) (Xu and Singh, 2000). (3) The combinational type requires temperature, radiation, wind speed, relative humidity, vapor pressure, etc. (Vicente-Serrano et al., 2014; Allen, 1998). All methods in these three categories incorporate several assumptions resulting in significant differences in their estimates (Lu et al., 2005).

In hydrological models, PET directly influences actual evapotranspiration (AET) and consequently impacts the estimation of infiltration, runoff and total water storage. In hydrological models, AET is estimated by either separately determining water surface evaporation, soil evaporation, and vegetation transpiration and then combining these based on land use patterns or by first assessing potential evapotranspiration and subsequently adjusting it to actual evapotranspiration using the soil moisture extraction function (Zhao et al., 2013). AET, being a key component of the water balance, affects the estimation of other water balance components (Q and TWS). Hence, uncertainty in PET estimation influences the quantification of change in water cycle components.

Many studies have investigated the sensitivity of the hydrological model output to PET. Oudin et al. (2005) evaluated 27 PET methods with four hydrological models concluding that PET is insensitive to runoff generation, with similar conclusions made by Aouissi et al. (2016); Birhanu et al. (2018). Assessment of four PET methods with two monthly hydrological models reported that runoff is unaffected by the PET method, whereas AET and total water storage depend on the PET method (Bai et al., 2016). The study also concluded that calibration against the runoff is the main cause of PET insensitivity, and AET and total water storage compensate for it. In contrast to previous studies, Ndiaye et al. (2024) compared 21 PET methods for runoff estimation with three conceptual lumped hydrological models (GR4J, GR5J, and GR6J) in the Senegal River Basin, stating that



55 better performance shown by combinational type methods. Similarly, Pimentel et al. (2023) compared three PET methods for
their accuracy in simulating runoff and AET in the large-scale hydrological model (HYPER model). They found that Hargreaves-
Samani performed best in the Amazonas, central Europe, and Oceania, and Priestley-Taylor in higher latitudes. These studies
focus on the sensitivity and choice of PET methods in estimating hydrological components. While these findings reveal how
PET methods can impact the magnitude of hydrological components, the impact of PET method selection on changes in these
60 hydrological components is not often investigated. Temporal changes in these hydrological components are crucial for climate
change mitigation, water availability, energy availability, and agricultural produce.

Trends in PET and its implication on hydrological components (AET) are examined by Anabalón and Sharma (2017). They
compare trends in six PET and AET datasets, mainly estimated by the Penman-Monteith or Priestley-Taylor PET method.
They found that PET trends were highly correlated with AET trends in energy-limited regions, while the AET trends were
65 closely correlated with precipitation trends in water-limited regions. Additionally, they reported that PET and AET trends were
inversely related in certain cases, mainly due to the prevailing influence of precipitation trends on AET trends. Similarly, Liu
et al. (2022) identified a strong positive relationship between PET and AET changes in most global regions and an inverse
relationship with total water storage change. The study is limited by using only the Penman-Monteith approach for PET and
global datasets for AET and total water storage change. The inconsistency and lack of coherence between existing PET and
70 AET datasets often necessitate using a single PET method compared to various AET datasets. Furthermore, previous studies
have primarily focused on one-to-one trend comparisons than comprehensive analysis of all hydrological cycle components,
including Q and TWS. Thus, research is needed to explore the impact of changes in PET methods on changes in different
hydrological components of hydrological models.

In this study, our objective is to assess the trends of PET using 12 different PET methods and their influence on the trend
75 of hydrological components (runoff; Q, AET, and total water storage; TWS) across 553 European catchments. To assess the
agreement between changes in different PET methods and corresponding hydrological components. The mesoscale hydro-
logical model (mHM) is used to evaluate the influence of changes in different PET methods, from simple to most advanced
approaches, on hydrological components across a range of European catchments. We chose a concurrency index to assess
agreement between the PET method and hydrological components at each catchment. The data concurrency index is used to
80 compare directions between different datasets (Anabalón and Sharma, 2017). In our research, we use it to examine directional
changes in PET estimates, AET, Q, and TWS across each catchment.

2 Methods and data

2.1 Study area and catchment classification

This study examines 553 catchments across Europe, covering all types of European climates. The selected catchment's sizes
85 vary from 500 km² to 252 000 km² and they are divided into three categories based on the aridity index: energy-limited, mixed,
and water-limited (Figure 1a). This classification is based on the aridity index (AI), estimated as the ratio of mean PET to mean
PRE, a widely used metric that quantifies the dry or wet state of the catchment (Zhang et al., 2016; Massari et al., 2022). In



our approach, which involves the application of multiple PET methods, a catchment is considered energy-limited if the AI is less than one for all the PET methods. Similarly, a catchment is water-limited if all PET methods report AI greater than one. If AI values appear to be both above and below one, depending on the PET method used, then the catchment is assigned to the mixed category (Figure 1b). This classification allows us to distinguish the differences in magnitudes of PET and the other key hydrological components among the catchments (Figure 1c). By employing this methodology out of 553 catchments, we find 189 catchments being energy-limited, 34 water-limited, and the rest 330 belong to the mixed category.

2.2 Meteorological and geomorphological data

The Ensemble Meteorological Dataset for Planet Earth (EM-Earth; Tang et al., 2022) and ERA5-land (Hersbach et al., 2020) were used to calculate different PET estimates and run the mesoscale Hydrological Model (mHM; Samaniego et al., 2010; Kumar et al., 2013). EM-Earth dataset is generated based on the observed station data (SC-Earth) and ERA5 data. It incorporates a novel optimal interpolation technique and considers the temporal inconsistencies between the station and reanalysis data (Tang et al., 2022). ERA5-land dataset is a reanalysis data product created by the European Centre for Medium-Range Weather Forecasts (ECMWF) and has been widely used in numerous hydrological modeling studies (Muñoz-Sabater et al., 2021). Both datasets are available at $0.1^\circ \times 0.1^\circ$ spatial resolution, but EM-Earth has hourly as well as daily time step, while ERA5-land is at hourly scale.

In our analysis, we use daily temperature and precipitation from EM-Earth, and radiation (long- and short-wave), surface pressure, and wind components (U and V) from ERA5-Land for the period 1980–2019 (Table 1). They are homogenized to daily temporal scale and $0.125^\circ \times 0.125^\circ$ spatial scale to be compatible with the previous simulations run by mHM (Pohl et al., 2023; Fang et al., 2024). Homogenization using the nearest neighbor technique and necessary mathematical operations (appropriate unit conversion of datasets) are performed using the Climate Data Operator (CDO; Schulzweida, 2022).

Morphological data such as Leaf Area Index (LAI), soil properties, and terrain characteristics (such as flow direction, flow accumulation, slope, and aspect) are sourced from mHM European database (Rakovec et al., 2016). This database originally utilized data from different sources, such as soil properties from the International Soil Reference and Information Centre (ISRIC), terrain characteristics from the U.S. Geological Survey (USGS) and the National Geospatial-Intelligence Agency (NGA), LAI from Global Inventory Modeling and Mapping Studies (GIMMS) and Land cover from Global Land Cover (GlobCover) by European Space Agency (ESA). CO₂ concentration is sourced from Cheng et al. (2022), which is reconstructed from the Carbon Dioxide Information Analysis Center (CDIAC) data.

2.3 Methodology

2.3.1 PET methods/formulations

We incorporate 12 PET methods at a daily scale from all three categories of estimation: temperature, radiation, and combinational methods (Table 2). Most temperature-based methods use only daily average temperature (Thorntwaite, Oudin, Hamon, Jensen-Haise, Mcguinnes-Bordne, Blaney-Criddle), while Baier-Robertson employs minimum and maximum daily

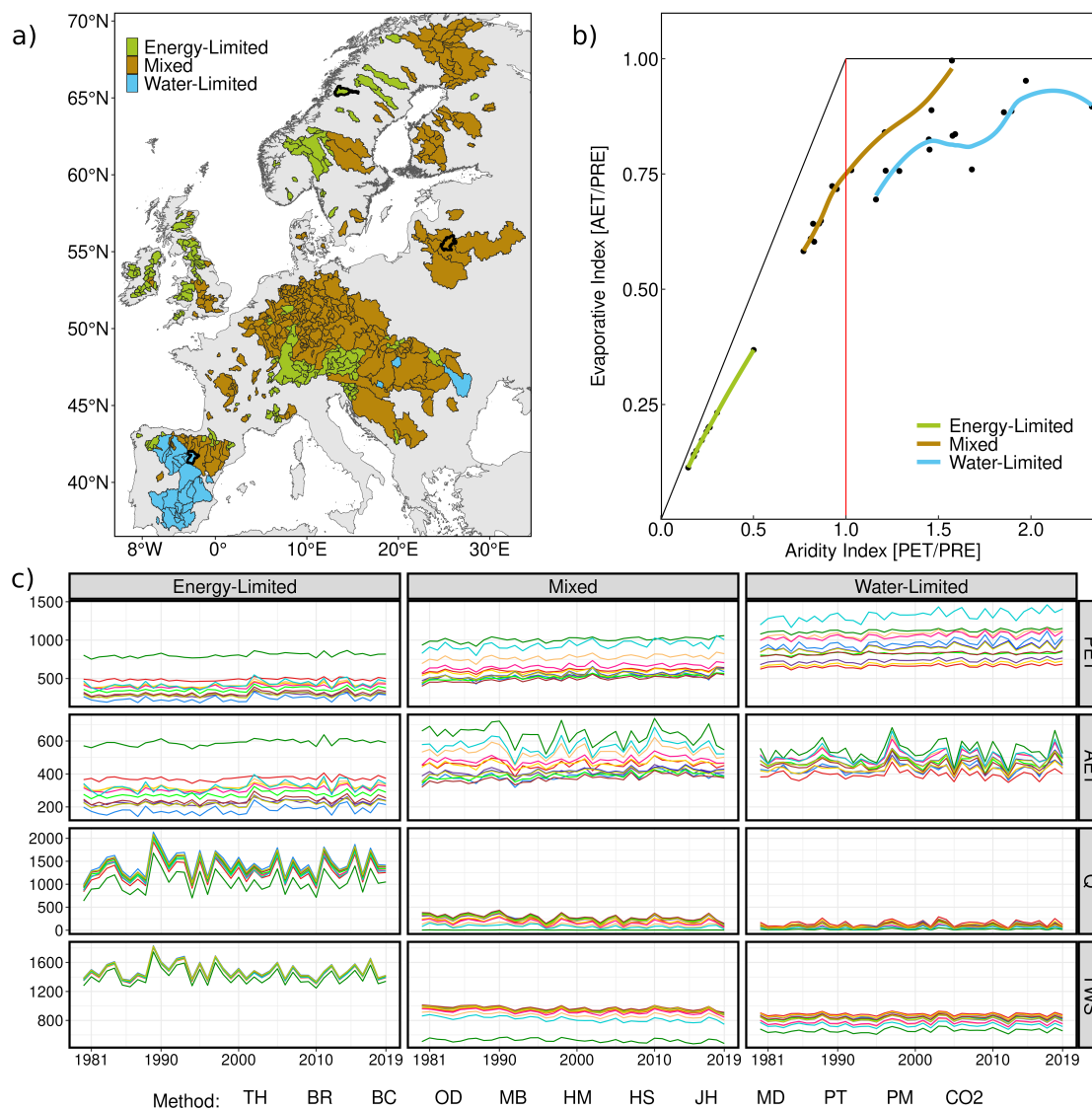


Figure 1. Catchment classification to energy-limited, mixed, and water-limited categories. a) Catchment locations; black borders indicate a representative catchment of each category. b) Classification example within the Budyko space for the representative catchments. c) Annual time series of hydrological components corresponding to each representative catchment and PET estimation method (TH: Thornthwaite, BR: Bair-Robertson, BC: Blaney-Criddle, OD: Oudin, MB: McGuinness-Borden, HM: Hamon, HS: Hargreaves-Samani, JH: Jensen-Haise, MD: Milly-Dunne, PT: Priestley-Taylor, PM: Penman-Monteith, CO₂: Modified Penman-Monteith accounts CO₂). All units are in mm year⁻¹.

120 temperature and Hargreaves-Samani uses minimum, maximum, and average daily temperature. Some of them also include an extraterrestrial radiation term in their formulation. However, since this extraterrestrial radiation term is calculated based on latitudinal information, only temperature data is required to calculate PET. We utilize only one radiation-based method, Milly-Dunne PET that requires only net radiation data to estimate PET. The combinational type includes the PET methods with a



Table 1. Summary of meteorological and morphological data. PRE is Precipitation, T_{avg} is average air temperature, T_{range} is the temperature range, which is the difference between maximum and minimum air temperature, T_{dew} is dew point temperature of air, SW is Short wave radiation, LW is longwave radiation, U is eastward component of wind speed at 10 m, V is northward component of wind speed at 10 m, ConCO_2 is CO_2 concentration

Variable	Temporal Scale	Spatial Scale	Record length	Source	Reference
Meteorological data					
PRE	Hourly/Daily	$0.1^\circ \times 0.1^\circ$	1950–2019	EM-Earth	Tang et al. (2022)
T_{avg}	Hourly/Daily	$0.1^\circ \times 0.1^\circ$	1950–2019	EM-Earth	Tang et al. (2022)
T_{range}	Hourly/Daily	$0.1^\circ \times 0.1^\circ$	1950–2019	EM-Earth	Tang et al. (2022)
T_{dew}	Hourly/Daily	$0.1^\circ \times 0.1^\circ$	1950–2019	EM-Earth	Tang et al. (2022)
SW	Hourly	$0.1^\circ \times 0.1^\circ$	1950–2022	ERA5-land	Muñoz-Sabater et al. (2021)
LW	Hourly	$0.1^\circ \times 0.1^\circ$	1950–2022	ERA5-land	Muñoz-Sabater et al. (2021)
U	Hourly	$0.1^\circ \times 0.1^\circ$	1950–2022	ERA5-land	Muñoz-Sabater et al. (2021)
V	Hourly	$0.1^\circ \times 0.1^\circ$	1950–2022	ERA5-land	Muñoz-Sabater et al. (2021)
Other data					
ConCO_2	Annual	$0.1^\circ \times 0.1^\circ$	1950–2022	–	Cheng et al. (2022)
LAI	monthly	$1/512^\circ$	static	GIMMS	Tucker, Pinzon, and Brown (2004)
Soil properties	–	$1/512^\circ$	–	SoilGrids	ISRIC - World SoilInformation (2017)
Land cover	static	$1/512^\circ$	static	GlobCover	Arino et al. (2012)
DEM (+ derivatives)	static	$1/512^\circ$	static	GMTED2010	USGS and NGA (2018)
Geology	static	$1/512^\circ$	static	GLiM	Hartmann and Moosdorf (2012)

stronger physical basis (Penman-Monteith, Priestley-Taylor). They employ more variables than the temperature- and radiation-
 125 based methods to estimate various physical terms such as relative humidity, vapor pressure, saturation vapor pressure, slope
 of vapor pressure curve, etc. In our analysis, all these physical terms are estimated according to Allen (1998). Additionally,
 in combinational category, we use the modified Penman-Monteith (CO_2) method, which accounts for temporal variation in
 changing carbon dioxide concentrations. Formulation details (mathematical equations and associated constants) of each PET
 method are provided in Table A1.

130 2.3.2 mesoscale Hydrological Model (mHM)

mHM is a hydrological model which explicitly accounts for sub-grid variability of hydrological processes (Samaniego et al.,
 2010; Kumar et al., 2013; Thober et al., 2019). mHM has been successfully applied and tested in more than 1000 Euro-
 pean basins ranging in size from 4 km^2 to more than $100\,000 \text{ km}^2$ at various spatial resolutions or grid cell size (1–100 km)
 (Samaniego et al., 2010; Kumar et al., 2013; Rakovec et al., 2016, 2019; Shrestha et al., 2024). Additionally, the model is
 135 currently applied at the global scale with comparable and sometimes even improved model performance with respect to other
 large-scale hydrological models (Samaniego et al., 2019). mHM demonstrates robust performance and applicability across



Table 2. List of PET methods and required input data. T_{\max} is maximum air temperature ($^{\circ}\text{C}$), T_{\min} is minimum air temperature ($^{\circ}\text{C}$), Pr is surface pressure (pa), R_n is net radiation (J/m^2), u_2 is the wind speed at 2m from the surface (m/s), Con_{CO_2} is CO_2 concentration (ppm)

Type	Method name	Method abbreviation	Required input	References
Temperature	Hargreaves-Samani	HS	T_{\max} , T_{\min} , T_{avg}	George H. Hargreaves and Zohrab A. Samani (1985)
	Thornthwaite	TH	T_{avg}	Thornthwaite (1948)
	Oudin	OD	T_{avg}	Oudin et al. (2005)
	Hamon	HM	T_{avg}	Hamon (1961)
	Baier-Robertson	BR	T_{\max} , T_{\min}	Bai et al. (2016)
	Jensen-Haise	JH	T_{avg}	Jensen and Haise (1963)
	McGuinness-Borden	MB	T_{avg}	McGuinness and Bordne (1972)
	Blaney-Criddle	BC	T_{avg}	Blaney (1952)
Radiation	Milly-Dunne	MD	R_n	Milly and Dunne (2016)
Combinational	Priestley-Taylor	PT	T_{avg} , Pr , R_n	Priestley and Taylor (1972)
	Penman-Monteith	PM	T_{\max} , T_{\min} , T_{avg} , T_{dew} , Pr , u_2 , R_n	Penman (1948)
	Penman Monteith[CO_2]	CO_2	T_{\max} , T_{\min} , T_{avg} , T_{dew} , Pr , u_2 , R_n , Con_{CO_2}	Yang et al. (2019)

Europe (Kumar et al., 2020). It is also one of the several large scale hydrological models, which were used by the WMO for their annual State of Global Water Resources reports (World Meteorological Organization (WMO), 2023).

We run mHM over 553 European catchments, using the meteorological data from EM-Earth and the 12 different PET estimation methods. Overall, 6 636 mHM simulations are performed for all the study basins. The basins were not calibrated for the each PET method to access their true response in hydrological cycle components. All meteorological forcings were kept constant with only varying PET estimate. To calculate TWS, we aggregate soil moisture at different layers, canopy interception storage, snowpack, groundwater levels, sealed area reservoirs, and unsaturated zone reservoirs at each grid cell and time step. The hydrological components (AET, Q, TWS) and PET are averaged over the catchment area and monthly time steps.

2.3.3 Trend analysis

We use Theil-Sen's slope method to calculate the magnitude and direction of linear change in PET, AET, Q, and TWS (Sen, 1968). Sen's slope is non-parametric and insensitive to outliers and types of distribution. Due to its robust application, this method is widely used in hydrology, climate, and environmental-related studies (Anabalón and Sharma, 2017; Thackeray et al., 2022). It accounts for all possible pairs of data points from a time series and finds the median value as the slope magnitude. Eq. 1 and 2 shows the calculation steps of Sen's slope:



$$S_k = \frac{X_j - X_i}{t_j - t_i} \quad \text{where } 1 \leq i < j \leq n \quad (1)$$

$$S_{med} = \begin{cases} S_{[\frac{n+1}{2}]} & \text{if } n \text{ is odd} \\ \frac{S_{[\frac{n}{2}]} + S_{[\frac{n+2}{2}]}}{2} & \text{if } n \text{ is even,} \end{cases} \quad (2)$$

where S_k is the linear slope for pair X_i and X_j , S_{med} is the median slope, X_i and X_j are data points from periods t_i and t_j , n is the number of data points in time series. Positive S_{med} represents a positive trend, with the magnitude indicating the rate of increase. Similarly negative S_{med} represents a negative trend, with the magnitude indicating the rate of decrease.

Here, we use the *trend* R package to estimate Sen's slope over a 40-year period from 1980 to 2019 at annual and seasonal (winter, spring, summer, and autumn) scales for each catchment.

2.3.4 Modified Data Concurrence Index (DCI)

The Data Concurrence Index quantifies the level of concurrence between the significant trends in different datasets of the same variable Anabalón and Sharma (2017). We modified this index by considering only directional information of corresponding slopes irrespective of trend significance i.e., counting the overall positive and negative slope occurrences. The adjustment was made to include all trend estimates from the PET methods. The Modified Data Concurrence Index (DCI) can be described as in Eq. 3:

$$DCI = \frac{1}{ND} \sum_{i=1}^{ND} \frac{S_i}{abs(S_i)}, \quad (3)$$

where DCI is the Modified Data Concurrence Index, ND denotes the number of datasets, and S_i is the magnitude of the slope.

The positive DCI represents a higher number of positive slopes than negative slopes and vice-versa. For instance, a DCI of 1 for AET and Q implies positive change for all the PET methods. Similarly, a DCI of -1 for AET and Q implies a negative change for all the PET methods. A DCI of 0.5 indicates that nine out of 12 methods, or 75% of the methods, show a positive change, and similarly, a DCI of -0.5 indicates that nine out of 12 methods show a negative change, or 75% of the methods. A DCI of zero denotes an equal number of positive and negative slopes (six positive and six negative). Our analysis estimates DCI from PET, AET, Q, and TWS slopes at annual as well as seasonal scales.



3 Results

3.1 Trend comparison of PET methods at annual scales

175 To quantify the long-term changes in hydrological cycle components, we used the Theil-Sen slope method. Changes in PET
depend on the choice of PET method selection (Figure 2). Considerable variability is observed among the PET methods, with
median trends ranging from slightly positive to 6 mm year^{-1} during the 1980–2019 period. The Jensen-Haise method shows
the highest trend among all methods across different catchments. In energy-limited catchments, a positive trend in PET is
observed across all methods, except Penman-Monteith and Penman-Monteith[CO₂] The median trend for each PET method is
180 positive, ranging from 1 mm year^{-1} to 2 mm year^{-1} . In mixed catchments, most PET methods reflect a positive trend, though
a few catchments using the Penman-Monteith[CO₂] method exhibit a slight negative trend. All PET methods exhibit a positive
trend in water-limited catchments, except the energy-based Milly-Dunne method. Overall variability in trend estimates of PET
methods decreases from energy-limited to mixed and water-limited catchments.

AET trends closely follow PET trends across all catchment categories (Figure 2). In energy-limited catchments, all PET
185 methods show a positive trend in terms of median values. However, a few catchments in this category reveal a slight neg-
ative change for the Blaney-Criddle, Jensen-Haise, Milly-Dunne, and Priestley-Taylor methods. For mixed catchments, the
median trend is positive for all PET methods except Blaney-Criddle. The negative trends are similar to those in energy-limited
catchments. Overall, the trend patterns for energy-limited and mixed catchments are similar to the trends in PET for these
catchments, regardless of trend magnitude, with a few exceptions such as Blaney-Criddle and Jensen-Haise (Figure S10). In
190 water-limited catchments, both positive and negative trends in AET are observed. The pattern remains similar to PET trends
with a few exceptions, such as Blaney-Criddle.

The long-term trends in Q are relatively insensitive compared to that of the PET for energy-limited and mixed catchment
categories (Figure 2). Despite the positive median, a substantial fraction of catchments exhibit a negative trend in energy-
limited catchments. In contrast, all methods show negative trends in mixed catchments with numerous catchments maintaining
195 a positive trend. In water-limited catchments, there is variability in PET methods; for instance, Milly-Dunne has a larger trend,
whereas Blaney-Criddle shows the lowest trend. Even though PET methods are insensitive in Q , variability exists among the
PET methods within each catchment category.

TWS shows sensitivity to PET methods in water-limited and mixed catchments, whereas energy-limited catchments re-
main rather insensitive (Figure 2). In energy-limited catchments, all PET methods have a negative trend corresponding to
200 the median; however, a substantial fraction of catchments exhibit a positive trend. Mixed catchments show similar results.
Temperature-based methods exhibit larger variability than radiation and combination types in mixed catchments. In water-
limited catchments, PET methods show both positive and negative trends, with negative trends close to zero. The Blaney-
Criddle, Hargreaves-Samani, and Milly-Dunne methods show large positive trends. Trend estimates based on Blaney-Criddle
method demonstrate large variability as compared to other PET methods in the mixed and water-limited categories.

205 Each PET method results in different trends in hydrological components (AET, Q , and TWS) for all catchment categories,
except for energy-limited catchments where Q and TWS show insensitivity to PET methods. The trend magnitude of PET



is reduced in that of AET trend, but the overall pattern of PET methods matches well with PET in all categories. In energy-limited catchments, PET methods are insensitive to Q and TWS, while in mixed and water-limited categories, Q and TWS exhibit varying trends. There is no single PET method that shows a consistently higher or lower trend in all the hydrological components.

3.2 Trend comparison of PET methods at seasonal scales

Hydrological cycle components exhibit considerable variability in trends across different seasons. In the summer season (JJA), nearly all PET methods demonstrate a positive trend for PET across all catchment categories, except for the Milly-Dunne method in water-limited catchments (Figure 3). The Jensen-Haise method has the highest trend and the greatest variability among all PET methods across each catchment category. Notable variability is observed among PET methods in water-limited catchments. The winter season exhibits the lowest trends, whereas the autumn season demonstrates comparable trends with summer for PET (Text S2). The summer season is the primary contributor to the annual trends in PET across all catchment categories (Figure S12). The trend pattern of AET in the winter season is similar to PET, while slight differences are observed in the spring and summer seasons (Text S2). AET in the summer season, energy-limited and mixed catchments typically exhibit an overall positive trend. The trend pattern among PET methods is consistent with the PET trends observed in energy-limited catchments. The Jensen-Haise method exhibits greater variability for both catchment types. However, despite the positive trend in PET, all PET methods reveal a negative trend in AET, with Blaney-Criddle displaying the highest negative trend, followed by Jensen-Haise. For AET, the summer season significantly contributes to the annual trends in both energy-limited and water-limited catchments. In contrast, for mixed catchments, both spring and summer seasons play a more substantial role, depending on the PET method (Figure S12).

In summer, Q remains largely insensitive to changes in PET method trends across all catchment categories, with slight variability among PET methods within each catchment category (Figure 3). A similar result is observed for the winter, spring, and autumn seasons are discussed in the supplementary information (Text S2). For energy-limited catchments, the trend in Q across different PET methods remains close to zero. For mixed catchments, almost all methods demonstrate a negative trend with varying trend magnitude, with Blaney-Criddle registering the least negative trend (Figure 3). Similarly, for water-limited catchments, Q shows insensitivity to PET method selection. However, radiation and combination methods reflect a positive trend corresponding to PET methods, whereas temperature-based methods exhibit both positive and negative trends in Q (Figure 3). For Q, distinct patterns are observed in the primary contributors to annual trends. In both water-limited and mixed catchments, spring is the most contributing season. In contrast, for energy-limited catchments, the December and summer seasons are the main contributors, with their impact varying depending on the selected PET method (Figure S13). For TWS in summer, energy-limited and mixed catchments are largely insensitive to the PET method, except for Jensen-Haise, which shows a negative trend. Although there is slight variation among PET methods within each category, mixed behavior is observed in water-limited catchments (Figure 3). Some temperature-based methods, including Blaney-Criddle, McGuinness-Bordne, and Hargreaves-Samani, indicate positive trends, while others show negative trends. All combination-type methods exhibit negative trends for TWS in summer.

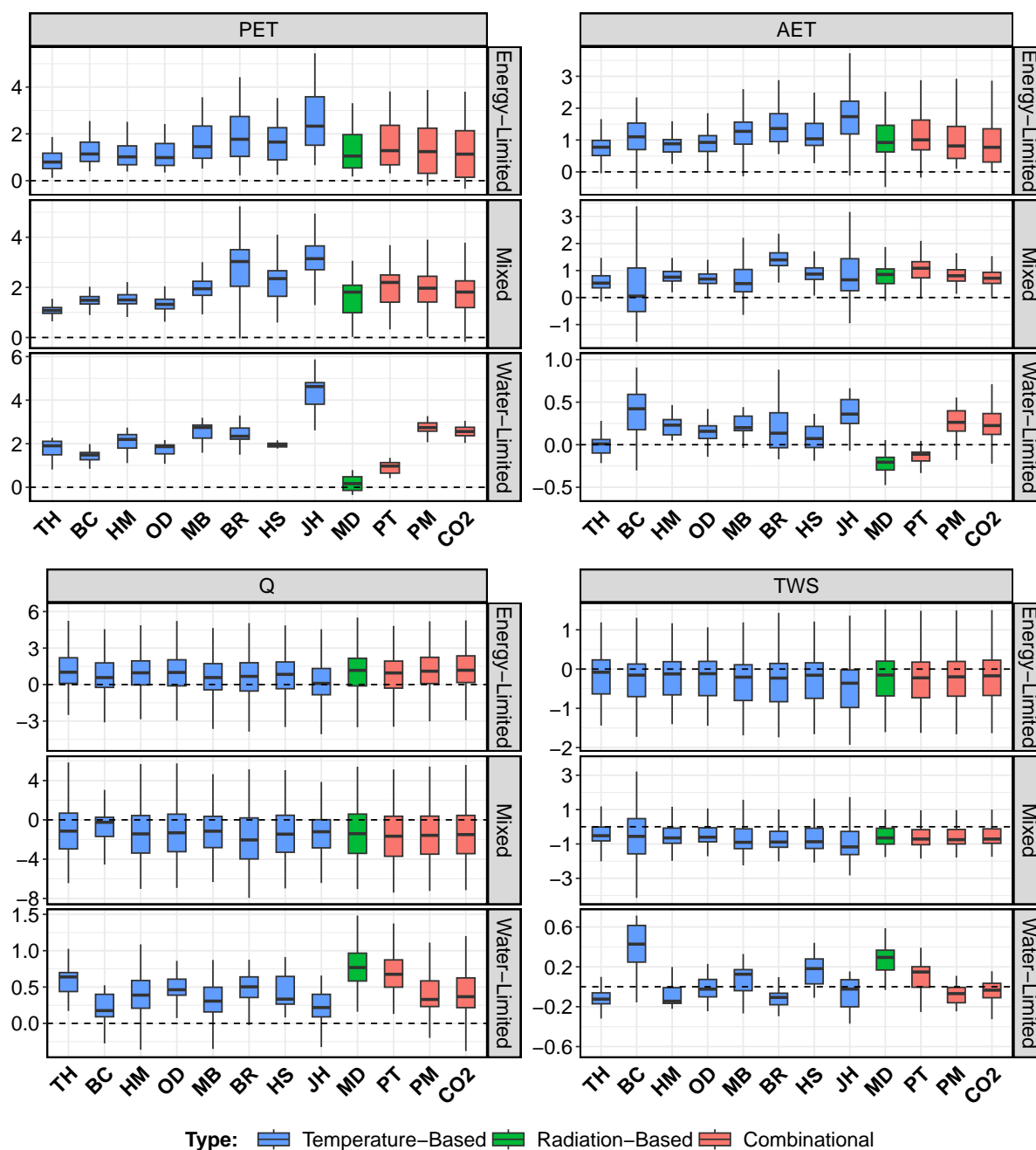


Figure 2. Boxplots represent the annual trends (mm year⁻¹) of different PET methods for PET, AET, Q, and TWS across various categories of catchment. The whiskers represent the 10th and 90th percentiles, and the box encompasses the 25th and 75th percentiles, with the median represented by middle line of the box. Abbreviations used for different PET methods are TH: Thornthwaite, BR: Bair-Robertson, BC: Blaney-Cridle, OD: Oudin, MB: McGuinness-Borden, HM: Hamon, HS: Hargreaves-Samani, JH: Jensen-Haise, MD: Milly-Dunne, PT: Priestley-Taylor, PM: Penman-Monteith, CO₂: Modified Penman-Monteith accounts CO₂.

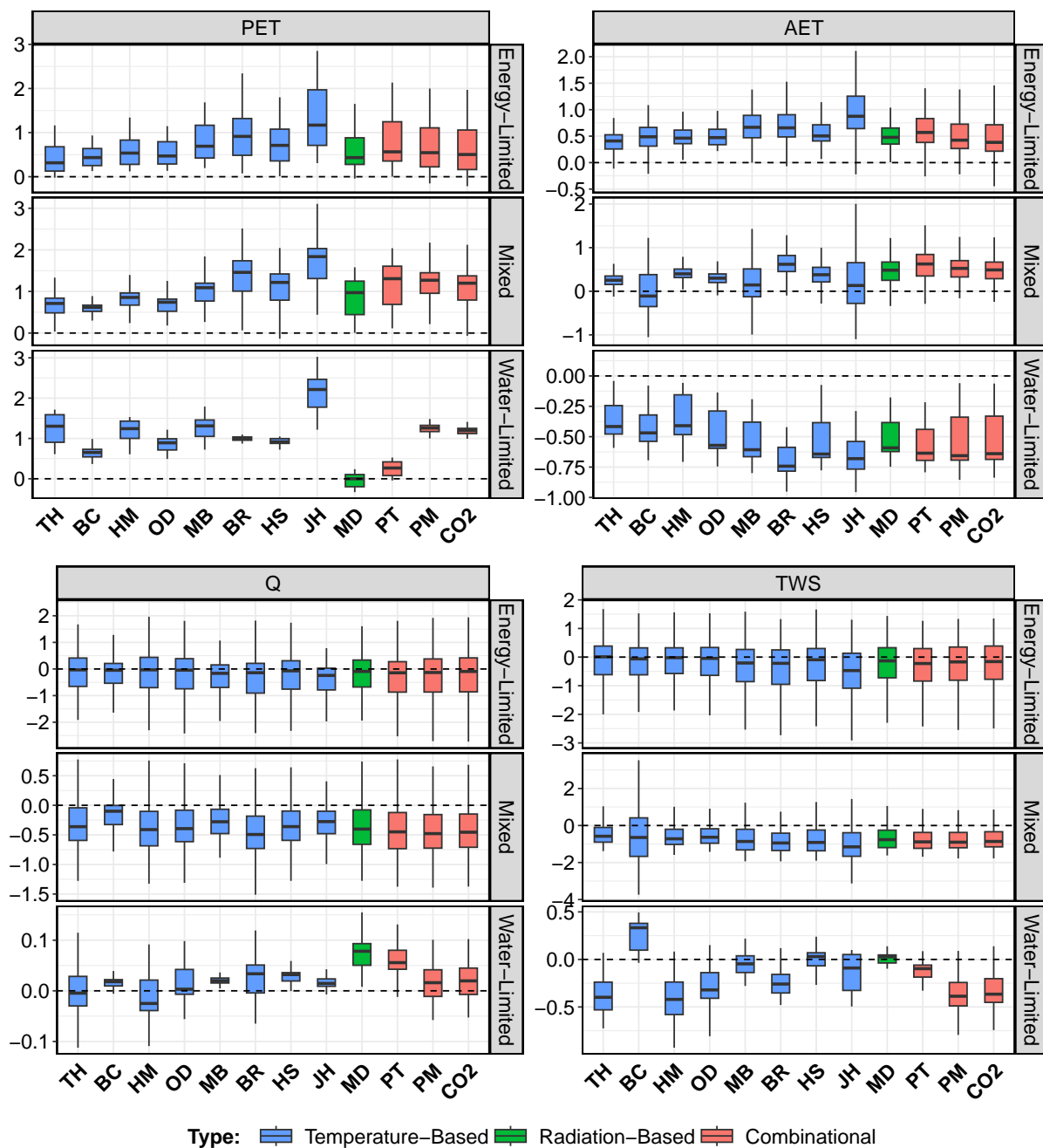


Figure 3. Boxplot represents the seasonal (summer season (JJA)) trends of different PET methods for AET, and Q across three categories of catchment: energy-limited, mixed, and water-limited. The whiskers represent the 10th and 90th percentiles, and the box encompasses the 25th and 75th percentiles, with the median represented by the black line within the box. Abbreviations used for different PET methods are TH: Thornthwaite, BR: Bair-Robertson, BC: Blaney-Cridde, OD: Oudin, MB: McGuinnes-Bordne, HM: Hamon, HS: Hargreaves-Samani, JH: Jensen-Haise, MD: Milly-Dunne, PT: Priestley-Taylor, PM: Penman-Monteith, CO₂: Modified Penman-Monteith accounts CO₂. Trend units are in mm seas⁻¹ year⁻¹.



3.3 Catchment-wise DCI distribution across annual and seasonal scales

Even though there is an strong agreement across different PET methods in annual PET and AET trends, the response in Q and TWS varies considerably (Figure 4). For PET, all catchments demonstrate strong positive DCI, indicating that a minimum of 75% of the PET methods exhibit a positive trend. A similar pattern is observed for AET, where higher positive DCI is noted in northern, central, and a few southern European catchments. Conversely, few catchments in southern Europe exhibit lower DCI values, with very few showing strong negative DCI. Q reflect strong positive agreement in southern catchments, with very few northern catchments showing positive DCI. The majority of northern catchments exhibit strong negative DCI. In contrast, central European catchments are marked by both strong positive and negative DCI, with few catchments with disagreement among PET methods. TWS shows disagreement among PET methods for southern, few central and northern European catchments. Most northern and central European catchments register strong negative agreement for PET methods. Overall, strong positive concurrence is observed between the PET methods for the directional agreement in the PET and AET trends, whereas mixed concurrency is seen for Q and TWS. Despite the higher positive DCI in PET, Q and TWS show higher negative DCI.

To better understand the annual changes of the level of concurrence between the trends, we decompose them into sub-seasonal values. Figure 5 shows that PET and AET demonstrate strong positive agreement across all seasons, whereas Q and TWS predominantly show strong negative agreement in central Europe, with evident regional variations. During spring, summer, and autumn, PET demonstrates a higher positive DCI across most catchments, reflecting an overall increasing trend among PET methods. In winter, central and southern European catchments have a high agreement, while others exhibit lower consistency. AET in central European catchments shows a higher positive DCI for winter, spring, and summer. However, northern European catchments reflect disagreement for AET across PET methods in winter, with a similar trend noted in some southern and central catchments during autumn. In southern Europe, AET demonstrates a strong negative DCI during summer. Across all seasons, Q shows a strong decreasing trend for all PET methods in most central European catchments. During spring and autumn, however, most southern catchments exhibit positive agreement among PET methods. In all seasons, central European catchments generally display strong negative DCI among PET methods for the TWS component. Southern European catchments exhibit a strong negative DCI in summer and a strong positive DCI in spring, while showing poor agreement in winter and autumn. Northern European catchments also experience a combination of positive and negative concurrence.

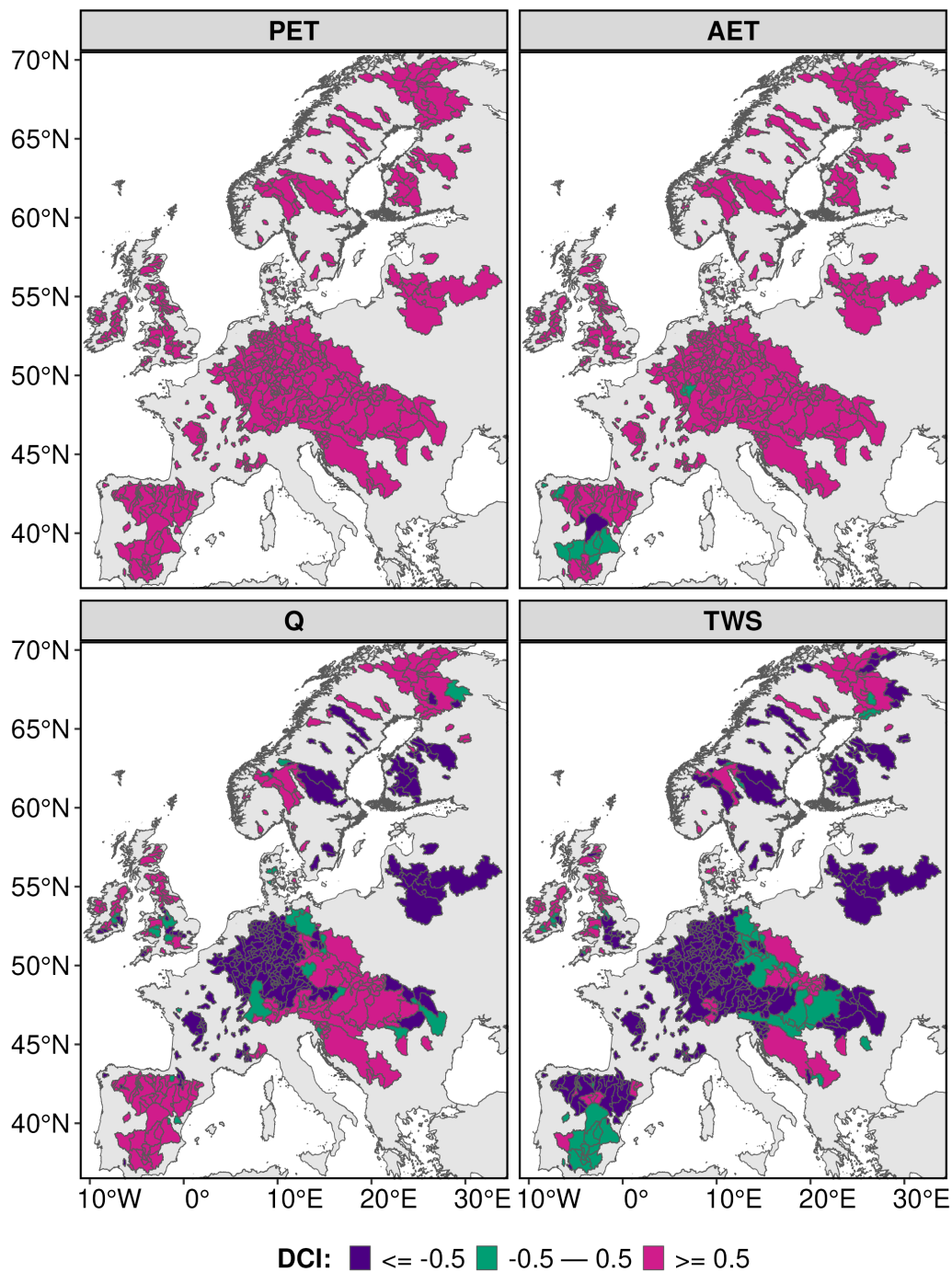


Figure 4. Spatial distribution of annual scale data concurrence index (DCI) for PET, AET, Q, and TWS. PET represents potential evapotranspiration, AET represents actual evapotranspiration, Q represents runoff at the outlet of the catchment and TWS represents total water storage.

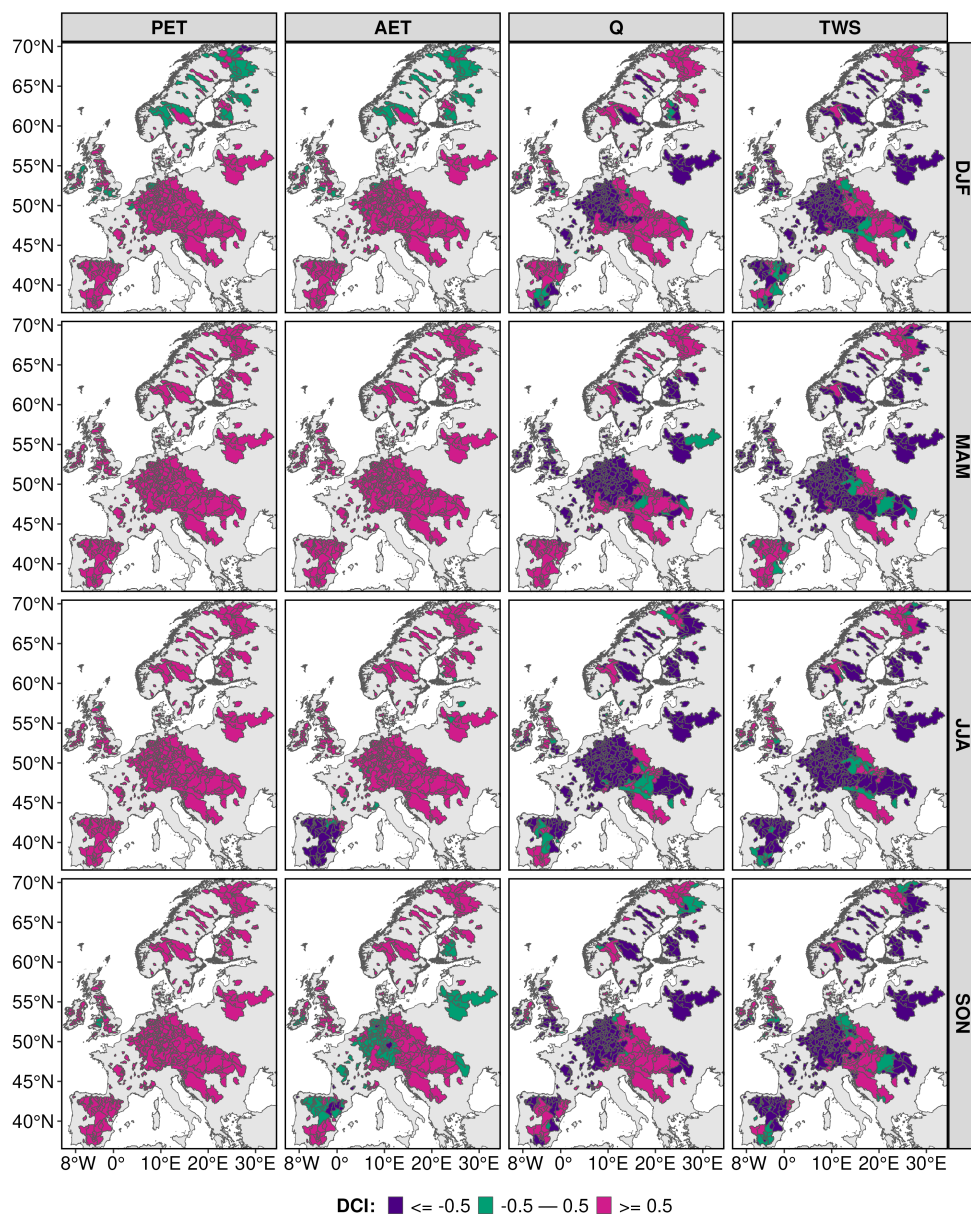


Figure 5. Spatial distribution of seasonal scale (winter (DJF), spring (MAM), summer (JJA), and autumn (SON)) DCI for PET, AET, Q, and TWS. Where DCI represents data concurrence index, PET represents potential evapotranspiration, AET represents actual evapotranspiration, Q represents runoff at the outlet of the catchment and TWS represents total water storage.



3.4 PET methods and combination of hydrological cycle components at annual and seasonal scales

In the previous section, we compared different PET method estimates and their impact on each hydrological component (AET, Q, and TWS), as well as the agreement between them. Here, we demonstrate the overall impact of PET methods on possible combinations of hydrological cycle component changes. Most catchments fall within the first five hydrological cycle combinations on annual scale (Figure 6). The Blaney-Criddle method has the highest catchment count for combinations featuring positive trends across all hydrological cycle components, while temperature-based methods account for more catchments than combinational methods (Figure 6). For combination featuring negative trends across all hydrological cycle components except AET, the Blaney-Criddle method and Bair-Robertson exhibit the lowest and highest catchment count respectively (Figure 6). For combinations showing positive trends in PRE and AET and negative trends in Q and TWS, temperature-based methods generally represent fewer catchments than combinational methods, with the Blaney-Criddle and Bair-Robertson methods exhibiting the lowest and highest counts, respectively (Figure 6). In cases with negative trends across all components, Blaney-Criddle and Bair-Robertson again demonstrate the highest and lowest catchment counts. The last five combinations of hydrological cycle in Figure 6 contribute very limited number of catchments, though the Blaney-Criddle method tends to capture more catchments within these combinations. Across combinations with positive AET and negative TWS trends, the Blaney-Criddle method accounts for the fewest catchments, while the Bair-Robertson method has the highest count.

Furthermore, we examine the seasonal patterns of PET method selection across different hydrological cycle component combinations. The initial five combinations remain consistent across seasons, while the last five are different due to the absence of certain hydrological combinations. In summer, for the combination featuring positive trends across all hydrological cycle components, temperature-based methods capture more catchments than radiation-based and combinational methods, with the Blaney-Criddle method accounting for the largest number (Figure S6). In cases where all components except AET show decreasing trends, combinational and radiation-based methods dominate, covering more catchments than temperature-based methods. For catchments with positive PRE and AET but negative Q and TWS trends, the Blaney-Criddle method demonstrates the least count. Combinational methods generally exhibit less variability in catchment counts, while temperature-based methods demonstrate more pronounced variations across hydrological cycle component combinations. In spring, the Blaney-Criddle method follows a similar pattern as of summer season, being the only method that shows decreasing trends in all hydrological cycle components (Figure S5). In the autumn (Figure S7), temperature-based methods again capture the largest number of catchments with positive trends in all components, while combinational methods have the fewest. For catchments with negative trends across all hydrological cycle components except AET, Baier-Robertson method shows the most catchments while the Blaney-Criddle method shows the least. Across all seasons, most catchments in summer exhibit positive trends for PRE and AET but negative trends for Q and TWS (Figure S6). In contrast, winter (Figure S4), spring (Figure S5), and autumn (Figure S7) generally exhibit decreasing trends in all components except AET.

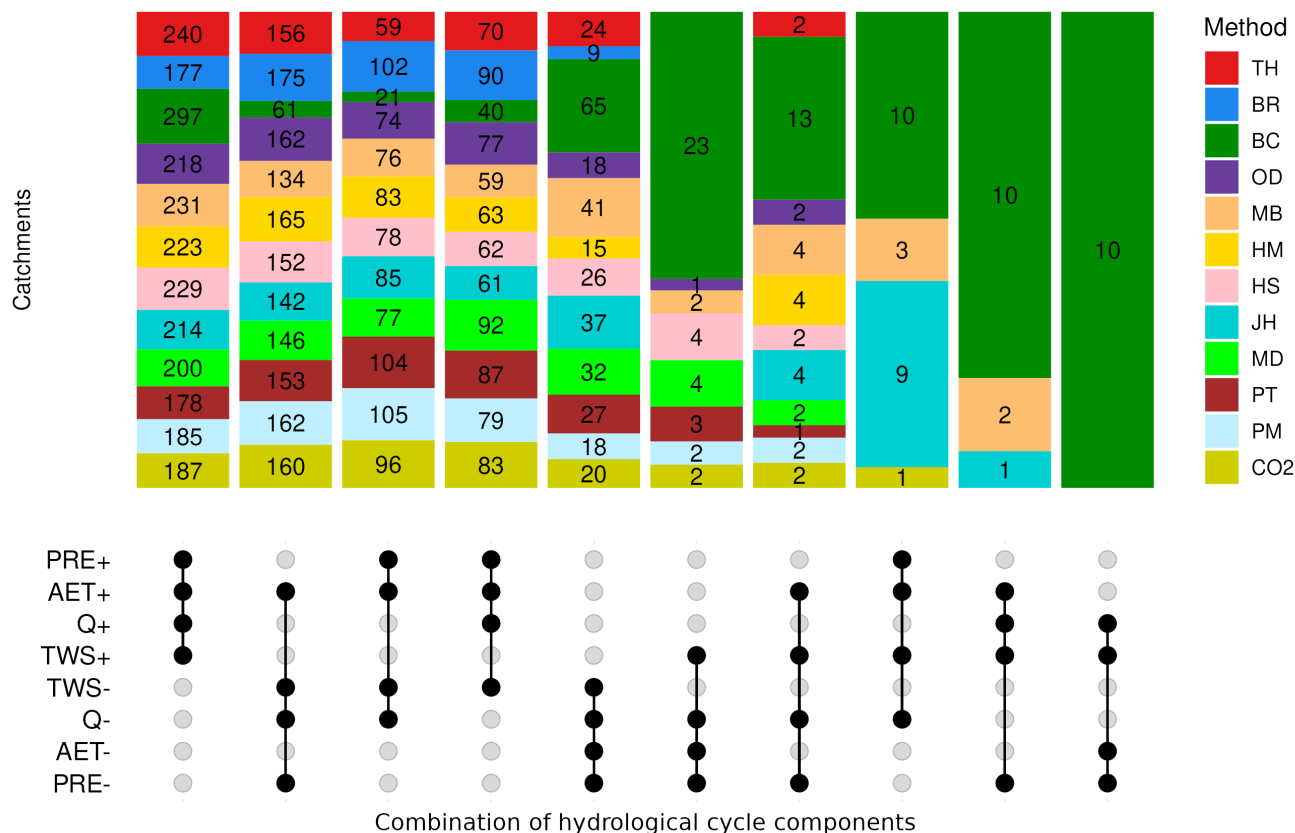


Figure 6. Combination of different hydrological cycle components and the corresponding influence of PET methods on an annual scale. PRE+, AET+, Q+, and TWS+ represent an increasing trend for PRE, AET, Q, and TWS respectively. Similarly, PRE-, AET-, Q- and TWS- represent a decreasing trend. Where PRE is precipitation, AET is actual evapotranspiration, Q is runoff and TWS is total water storage. Abbreviations used for different PET methods are TH: Thornthwaite, BR: Bair-Robertson, BC: Blaney-Criddle, OD: Oudin, MB: McGuinness-Borden, HM: Hamon, HS: Hargreaves-Samani, JH: Jensen-Haise, MD: Milly-Dunne, PT: Priestley-Taylor, PM: Penman-Monteith, CO₂: Modified Penman-Monteith accounts CO₂.

4 Discussion

The estimates from PET methods consistently show an upward trend over European catchments annually (Figure 2), which is in agreement with the work of Anabalón and Sharma (2017), who also reported such an increase across Europe using diverse PET datasets. The Jensen-Haise method consistently yields higher absolute values for European catchments, in agreement with Hanselmann et al. (2024) research in Poland. The Jensen-Haise method shows the highest trend in all categories. The Jensen-Haise method relies on temperature and extraterrestrial radiation data. Extraterrestrial radiation remains constant each year. Therefore, the observed trends are primarily driven by temperature variations. Shi et al. (2023b) found that Jensen-Haise trends align closely with Penman-Monteith, which is used as a benchmark for evaluating other PET methods. We observed



a notable distinction between the Jensen-Haise and Penman-Monteith PET methods. The differences in trends between these methods stem mainly from meteorological forcings. In the Jensen-Haise method, temperature is a significant factor in the trend. For Penman-Monteith, however, radiation is the main factor, followed by temperature, vapor pressure deficit, and wind speed (Maček et al. (2018)). The Milly-Dunne method consistently demonstrates the lowest trends in water-limited catchments. This trend, influenced by net radiation, remains lower in the south of Europe (Pfeifroth et al. (2018)). In the presented work, we do not perform sensitivity analyses of each PET method with meteorological forcings, as this falls outside the scope of the paper.

The AET trend is proportional to the PET trend in energy-limited and mixed catchments. In water-limited regions, there is not enough water to evaporate and it is mainly governed by available water (PRE) Bruno and Duethmann (2024). This results in a notable decline in AET when compared to PET. As reported by Anabalón and Sharma (2017), AET tends to correlate more closely with PET in energy-limited regions and with precipitation in water-limited regions. However, their analysis did not consider different PET methods but used various existing datasets instead. AET exhibits the same directional changes as precipitation at both annual and seasonal scales in water-limited catchments (Figure S9). Despite differences among catchment categories, PET methods demonstrate strong positive or negative agreement in AET trends.

In general, the runoff (Q) trend varies based on the PET method across water-limited catchments, whereas energy-limited and mixed catchment show insensitivity to PET method selection. This is in line with earlier work, e.g., Bai et al. (2015); Oudin et al. (2005); Seiller and Anctil (2016) who reported that runoff was generally insensitive to PET formulations. This insensitivity is primarily attributed to the calibration of hydrological models, where the impact of PET models is offset by the parameterization of the hydrological model. Surprisingly, even though we did not calibrate the hydrological model for individual PET methods, we observed insensitivity to PET methods in energy-limited and mixed catchments. This is primarily because the trend in precipitation is strongly correlated (Figure S11) with the trend in runoff (Q) (Berghuijs et al., 2017), which often outweighs the impact of PET (Anabalón and Sharma, 2017). The strong negative agreement between PET methods for runoff (Q) across central European catchments was due to their strong correlation with precipitation (Figure S9).

Total water storage (TWS) appears to be insensitive in energy-limited and mixed catchments, while it exhibits variability in the trend of different PET methods in water-limited catchments. Bai et al. (2016) observed that TWS in energy-limited catchments is more strongly impacted by PET than in water-limited catchments, though their study focused solely on Chinese catchments. More recently, Boeing et al. (2024) reported a decline in TWS over Germany, consistent with our findings that TWS decreases in energy-limited and mixed catchments for all PET methods. In hydrological models, TWS compensates for long-term changes, i.e., higher PET results in lower TWS in energy-limited catchments, whereas water-limited catchments are primarily governed by precipitation (Bai et al., 2016). This is in line of our findings on the opposite TWS trends relative to AET and a stronger agreement among PET methods in energy-limited and mixed catchments.

A large number of catchments across Europe exhibit positive changes in the hydrological cycle; however, variations exist depending on the PET methods employed. Teuling et al. (2019) found increasing PRE, AET and Q in central-west Europe, while these hydrological cycle components decreased in the Mediterranean region using the Penman method for PET estimation. Our results confirm that the Penman method identifies fewer catchments showing these trends compared to temperature-based PET methods. This variation will cause discrepancies in the conclusions of hydrological cycle intensification studies. Similarly,



many catchments demonstrate a drying hydrological cycle (positive change in AET and negative changes in Q, TWS, and PRE). The number of catchments demonstrating these trends varies depending on the choice of PET method. Massari et al. (2022) found that over Europe runoff deficit are more pronounced in water-limited regions due to increased AET, whereas energy-limited catchments exhibit smaller deficits. During these drying conditions, AET is further influenced by reductions in TWS (Massari et al., 2022).

Even though our study's experimental design varies from the global analysis of Pimentel et al. (2023), both utilize large-scale hydrological models at the basin scale. Pimentel et al. (2023) compare three different PET methods to choose the best PET method to estimate PET, AET, and Q in the hydrological model. Across Europe they reported that Jensen-Haise in northern Europe (energy-limited), Hargreaves in central (mixed), and Priestley-Taylor alongside Hargreaves-Samani in southern Europe (water-limited) perform better to estimate PET. For AET estimation, the Jensen-Haise method outperforms in northern Europe (energy-limited), while Hargreaves-Samani leads in central Europe (mixed) and Priestley-Taylor in southern Europe (water-limited). They also argue that Priestley-Taylor is predominantly the most effective method for runoff estimation. In our study, we found a consistently notable distinction between Jensen-Haise and Penman-Monteith across all catchment types for PET. Similarly, for AET, Jensen-Haise consistently shows higher trends than Penman-Monteith in both energy-limited and water-limited catchments. We observed that changes in energy-limited and mixed catchments are similar for runoff (Q) when using the Priestley-Taylor and Penman-Monteith methods. However, in water-limited catchments, Priestley-Taylor leads to greater changes than ones estimated by the Penman-Monteith method.

PET method selection impacts the hydroclimatic state of the catchment. The hydroclimatic state of a catchment is commonly classified into two categories water-limited and energy-limited catchments based on the aridity index. In our research, we introduce a third catchment category termed "mixed", which does not represent any physical basis. However, it underscores the crucial importance of PET method selection specifically for the mixed catchment category. For instance, using a PET method that consistently generates a higher PET estimate may change a catchment from energy-limited to water-limited, whereas a method that produces a lower PET estimate can shift it from water-limited to energy-limited. Similarly, Zhang et al. (2016) introduced a slightly different and not well-known classification called "equitant", which applies a single PET method to calculate the aridity index. Such variations could cause discrepancies in the results. For example, Kuentz et al. (2017) uses the Jensen-Haise method, Ajami et al. (2017) uses the Priestley-Taylor method, and Zhang et al. (2016) uses the Penman method to calculate the aridity index to classify catchments. We observed catchments shifting from the mixed to the energy-limited category after excluding PET methods that consistently overestimate PET. For instance, removing Blaney-Cridle, Jensen-Haise and McGuinness-Bordne, 42% of the total catchments shift from mixed category to energy-limited catchment category (Figure S8). Shifts in catchments, based on various combinations, are presented in Table S1.

Our study comes with certain limitations that pave the way for future research. First of all, it is limited by the uncertainty associated with the input data used to calculate the PET methods. However, previous detailed studies have investigated the uncertainties related to these data (Hua et al., 2020; Guo et al., 2017). They reported that PET methods are sensitive to their input data: temperature-based methods to temperature, radiation-based methods to radiation, and combination methods predominantly to both temperature and radiation, as well as to relative humidity and wind speed. Additionally, we limited our analysis



to one precipitation product to isolate the specific impact of the PET method. However, it is well known that precipitation is the most sensitive meteorological input, Voisin et al. (2008); Mazzoleni et al. (2019) have extensively studied the uncertainties related to precipitation. This identifies a potential gap for exploring the combination of precipitation with PET for accurate simulation of hydrological cycle components.

380 Often large-scale hydrological models use default parameterization. This research can be further extended by incorporating calibration for all three hydrological components (AET, Q, and TWS) in areas with data availability. This study is confined to temperate climate European catchments, and there is a potential gap in extending this research to arid and tropical climates, which could yield different and interesting results. Although the Modified Penman-Monteith method accounts for CO₂, it did not show substantial differences compared to the Penman method. Further exploration of this method, along with others, would
385 be interesting to assess their impact under changing climate conditions.

5 Summary and conclusions

Twelve PET methods were used to evaluate their impacts on changes in the components of the hydrological cycle using the mesoscale Hydrological Model (mHM). These methods were applied across 553 European catchments, which vary in size and include different European climate types. These catchments were classified as water-limited, energy-limited, and mixed
390 catchments based on their aridity index. To analyze changes in PET and hydrological components, we employed Sen's slope estimate, and to assess the agreement between different PET methods, we used the modified data concurrence index for the period 1980 to 2019. The results demonstrate that the choice of PET method can substantially affect changes in AET, Q, and TWS, especially in water-limited and mixed catchments, with smaller changes and greater variability observed in water-limited catchments on an annual scale. Seasonal variations in changes and agreement between PET methods were also observed, as
395 discussed in detail in sections 3.2 and 3.3. In general, there is agreement among the different methods that, since 1981, PET and AET are increasing over Europe, while runoff and total water storage exhibit mixed fluctuations depending on the method used and the catchment latitude. The key findings of our study are summarized as follows:

1. PET is increasing across European catchments. The majority of the PET methods indicate a positive trend in all categories of catchments, but the increase rates differ among the methods employed.
- 400 2. At the annual scale, the Jensen-Haise PET method stands out by consistently showing the highest trends for PET and AET across all catchment categories. The Milly-Dunne (energy-based) method is notable as the only one to exhibit a negative trend for water-limited catchments. Regarding Q and TWS, the PET methods display different changes and variability, with no method consistently showing either the lowest or highest trends for these hydrological components.
3. The trend patterns between PET and AET are similar across all methods for the hydrological cycle components. However,
405 Q and TWS do not exhibit the same pattern and appear to be less sensitive to choice of PET methods. Most PET methods agree on the trend direction for PET and AET, but in a few catchments, the trends for Q and TWS show an opposite



direction. The negative trends in Q and TWS are primarily due to negative precipitation trends, which have a stronger impact on these components in all catchment categories.

- 410 4. At the seasonal scale, PET methods reveal different trends for PET, with no method consistently showing the highest or lowest trends across all seasons. However, the Jensen-Haise method shows the highest PET trends during spring, autumn, and summer. AET trends follow a similar pattern to PET in all seasons. The PET methods show strong agreement on trend direction for central and southern European catchments, especially for PET, but there is less agreement for northern catchments in winter. Strong negative agreement is found for Q and TWS in summer and spring, while disagreement is observed for AET in central and southern catchments during autumn.
- 415 5. The summer season contributes more to the annual PET trends than any other season across all catchment categories. Similarly, for AET, the summer season has a higher contribution to the annual AET trend in energy-limited and water-limited catchments. For runoff (Q), the spring season contributes more in mixed and water-limited catchments. For TWS, the spring season has a higher contribution in energy-limited catchments.
- 420 6. Overall, The magnitude of trends varied between PET methods for PET and the hydrological components (Q, AET, and TWS). The use of a specific PET method in a hydrological model can notably affect studies focused on the hydrological cycle.
7. Precipitation is the primary factor influencing the trends of hydrological components and is responsible for the overall direction of hydrological cycle components (AET, Q, and TWS).

Our research demonstrates the critical role of PET method selection and its implications for quantifying fluctuations in the hydrological cycle. Our findings reveal that two methods notably deviate from the others. Specifically, the Jensen-Haise method shows higher trend values, while the Milly-Dunne method exhibits lower trends in water-limited catchments. Consequently, we recommend exercising caution when applying these methods as they appear to be outliers. Despite these variations, the PET methods generally agree that atmospheric moisture demand is increasing across Europe, reflecting recent shifts in temperature and radiation. Given the differences in trend magnitudes across methods, we encourage the use an ensemble of PET formula-
430 tions in the assessment of changes in the water cycle components. It allows us to capture a more comprehensive and reliable representation of hydrological trends.

Code and data availability.

The necessary data required to reproduce the final analysis and figures are available in the zenodo repository (<https://doi.org/10.5281/zenodo.14008649>). Codes used to analyze the results are publicly available in the GitHub repository (https://github.com/imarkonis/ithaca/tree/main/projects/pet_europe).
435



Author contributions.

VT: conceptualization, PET calculation, hydrological model simulations, postprocessing, formal analysis, and writing (original draft), YM: conceptualization, supervision, writing (review and editing) RK: conceptualization, writing (review and editing), JRT: writing (review and editing), MRVG: writing (review and editing), MH: writing (review and editing), OR: setup of
440 hydrological model, supervision, conceptualization, writing (review and editing).

Competing interests.

At least one of the (co)-authors is a member of the editorial board of Hydrology and Earth System Sciences.

Acknowledgements. This work was carried out within the project “Investigation of Terrestrial HydrologicAI Cycle Acceleration (ITHACA)” funded by the Czech Science Foundation (Grant 22-33266M). Computational resources were provided by the e-INFRA CZ project (ID:90254),
445 supported by the Ministry of Education, Youth and Sports of the Czech Republic. VT was also funded by the Internal Grant Agency (Project no: 2023B0008), Czech University of Life Sciences.

Appendix A: Potential Evapotranspiration formulation



Table A1. Formulations of PET methods. Where R_e is extraterrestrial radiation ($\text{MJ m}^{-2} \text{d}^{-1}$), λ is the latent heat of vaporization (MJ kg^{-1}), ρ is water density ($= 1000 \text{ kg m}^{-3}$), d_a is air density (kg m^{-3}), T_a is air temperature ($^{\circ}\text{C}$), T_d is dew point temperature ($^{\circ}\text{C}$), T_{\max} is maximum air temperature ($^{\circ}\text{C}$), T_{\min} is minimum air temperature ($^{\circ}\text{C}$), Δ is the slope of the vapor pressure curve ($\text{kPa } ^{\circ}\text{C}^{-1}$), γ is the psychrometric constant ($\text{kPa } ^{\circ}\text{C}^{-1}$), e_s is saturation vapour pressure (kPa), e_a is actual vapour pressure (kPa), u_2 is wind speed 2 m above the soil surface (m s^{-1}), R_s is net short-wave radiation ($\text{MJ m}^{-2} \text{d}^{-1}$), R_n is net incoming solar radiation ($\text{MJ m}^{-2} \text{d}^{-1}$), G is soil heat flux ($\text{MJ m}^{-2} \text{d}^{-1}$), RH is relative humidity (%), DL is day length (h d^{-1}), I is annual heat index, and CO_2 is carbon dioxide concentration (ppm).

Method	Formulation
Hargreaves Samani	$0.0023 \times \frac{R_e}{\lambda \times \rho} \times \sqrt{t_{\max} - t_{\min}} \times (t_{\text{avg}} + 17.8) \times 1000$
McGuinness-Bordne	$1000 \times \frac{R_e}{\lambda \times \rho} \times \frac{T_a + 5}{68}$
Hamon	$k \times 0.165 \times 216.7 \times \frac{DL}{12} \times \frac{e_s}{t_{\text{avg}} + 273.3}$
Oudin	$1000 \times \frac{R_e}{\lambda \times \rho} \times \frac{t_{\text{avg}} + 5}{100}$
Baier and Robertson	$0.157 \times t_{\max} + 0.158(t_{\max} - t_{\min}) + 0.109 \times R_e - 5.39$
Blaney-Criddle	$0.825 \times (0.46 \times t_{\text{avg}} + 8.13) \times \frac{100 \times DL}{365 \times 12}$
Thornthwaite	$16 \times \frac{DL}{360} \times \left(\frac{10 \times t_{\text{avg}}}{I} \right)^k$
Jensen-Haise	$1000 \times \frac{R_e}{\lambda \times \rho} \times \frac{T_{\text{avg}}}{40}$
Priestley and Taylor	$\frac{1.26 \times \Delta \times (R_n - G)}{\lambda \times \rho \times (\Delta + \gamma)}$
Milley-Dunne	$0.8 \times (R_n - G)$
Penman-Monteith	$\frac{0.408 \times \Delta \times (R_n - G) + \gamma \times \left(\frac{900}{T_{\text{avg}} + 273} \right) \times u_2 \times (e_s - e_a)}{\Delta + \gamma \times (1 + 0.34 \times u_2)}$
Modified Penman-Monteith	$\frac{0.408 \times \Delta \times (R_n - G) + \gamma \times \left(\frac{900}{T_{\text{avg}} + 273} \right) \times u_2 \times (e_s - e_a)}{\Delta + \gamma \times (1 + 0.34 \times (u_2 + 2 \times 10^{-4} \times ([CO_2] - 300)))}$



References

- Ajami, H., Sharma, A., Band, L. E., Evans, J. P., Tuteja, N. K., Amirthanathan, G. E., and Bari, M. A.: On the non-stationarity of hydrological
450 response in anthropogenically unaffected catchments: an Australian perspective, *Hydrology and Earth System Sciences*, 21, 281–294,
<https://doi.org/10.5194/hess-21-281-2017>, 2017.
- Allen, R. G., ed.: *Crop evapotranspiration: guidelines for computing crop water requirements*, no. 56 in *FAO irrigation and drainage paper*,
Food and Agriculture Organization of the United Nations, Rome, ISBN 978-92-5-104219-9, 1998.
- Anabalón, A. and Sharma, A.: On the divergence of potential and actual evapotranspiration trends: An assessment across alternate global
455 datasets, *Earth's Future*, 5, 905–917, <https://doi.org/10.1002/2016EF000499>, 2017.
- Aouissi, J., Benabdallah, S., Lili Chabaâne, Z., and Cudennec, C.: Evaluation of potential evapotranspiration assessment methods
for hydrological modelling with SWAT—Application in data-scarce rural Tunisia, *Agricultural Water Management*, 174, 39–51,
<https://doi.org/10.1016/j.agwat.2016.03.004>, 2016.
- Arino, O., Ramos Perez, J. J., Kalogirou, V., Bontemps, S., Defourny, P., and Van Bogaert, E.: *Global Land Cover Map for 2009 (GlobCover
460 2009)*, <https://doi.org/10.1594/PANGAEA.787668>, artwork Size: 40 data points Pages: 40 data points, 2012.
- Arnold, J. G., Srinivasan, R., Muttiah, R. S., and Williams, J. R.: LARGE AREA HYDROLOGIC MODELING AND ASSESSMENT
PART I: MODEL DEVELOPMENT, *Journal of the American Water Resources Association*, 34, 73–89, <https://doi.org/10.1111/j.1752-1688.1998.tb05961.x>, 1998.
- Bai, P., Liu, X., Liang, K., and Liu, C.: Comparison of performance of twelve monthly water balance models in different climatic catchments
465 of China, *Journal of Hydrology*, 529, 1030–1040, <https://doi.org/10.1016/j.jhydrol.2015.09.015>, 2015.
- Bai, P., Liu, X., Yang, T., Li, F., Liang, K., Hu, S., and Liu, C.: Assessment of the Influences of Different Potential Evapotranspiration Inputs
on the Performance of Monthly Hydrological Models under Different Climatic Conditions, *Journal of Hydrometeorology*, 17, 2259–2274,
<https://doi.org/10.1175/JHM-D-15-0202.1>, 2016.
- Berghuijs, W. R., Larsen, J. R., van Emmerik, T. H. M., and Woods, R. A.: A Global Assessment of Runoff Sensitivity to Changes in Pre-
470 cipitation, Potential Evaporation, and Other Factors, *Water Resources Research*, 53, 8475–8486, <https://doi.org/10.1002/2017WR021593>,
2017.
- Birhanu, D., Kim, H., Jang, C., and Park, S.: Does the Complexity of Evapotranspiration and Hydrological Models Enhance Robustness?,
Sustainability, 10, 2837, <https://doi.org/10.3390/su10082837>, 2018.
- Blaney, H. F.: *Determining water requirements in irrigated areas from climatological and irrigation data*, 1952.
- 475 Boeing, F., Wagener, T., Marx, A., Rakovec, O., Kumar, R., Samaniego, L., and Attinger, S.: Increasing influence of evapotranspiration on
prolonged water storage recovery in Germany, *Environmental Research Letters*, 19, 024047, <https://doi.org/10.1088/1748-9326/ad24ce>,
2024.
- Bruno, G. and Duethmann, D.: Increases in Water Balance-Derived Catchment Evapotranspiration in Germany During 1970s–2000s
Turning Into Decreases Over the Last Two Decades, Despite Uncertainties, *Geophysical Research Letters*, 51, e2023GL107753,
480 <https://doi.org/10.1029/2023GL107753>, 2024.
- Cheng, W., Dan, L., Deng, X., Feng, J., Wang, Y., Peng, J., Tian, J., Qi, W., Liu, Z., Zheng, X., Zhou, D., Jiang, S., Zhao, H., and Wang,
X.: Global monthly gridded atmospheric carbon dioxide concentrations under the historical and future scenarios, *Scientific Data*, 9, 83,
<https://doi.org/10.1038/s41597-022-01196-7>, 2022.



- Fang, B., Bevacqua, E., Rakovec, O., and Zscheischler, J.: An increase in the spatial extent of European floods over the last 70 years, *EGU*, <https://doi.org/10.5194/egusphere-2023-2890>, 2024.
- George H. Hargreaves and Zohrab A. Samani: Reference Crop Evapotranspiration from Temperature, *Applied Engineering in Agriculture*, 1, 96–99, <https://doi.org/10.13031/2013.26773>, 1985.
- Guo, D., Westra, S., and Maier, H. R.: Sensitivity of potential evapotranspiration to changes in climate variables for different Australian climatic zones, *Hydrology and Earth System Sciences*, 21, 2107–2126, <https://doi.org/10.5194/hess-21-2107-2017>, 2017.
- 490 Hamon, W. R.: Estimating Potential Evapotranspiration, *Journal of the Hydraulics Division*, 87, 107–120, <https://doi.org/10.1061/JYCEAJ.0000599>, 1961.
- Hanselmann, N., Osuch, M., Wawrzyniak, T., and Alphonse, A. B.: Evaluating potential evapotranspiration methods in a rapidly warming Arctic region, SW Spitsbergen (1983–2023), *Journal of Hydrology: Regional Studies*, 56, 101979, <https://doi.org/10.1016/j.ejrh.2024.101979>, 2024.
- 495 Hartmann, J. and Moosdorf, N.: The new global lithological map database GLiM: A representation of rock properties at the Earth surface, *Geochemistry, Geophysics, Geosystems*, 13, 2012GC004370, <https://doi.org/10.1029/2012GC004370>, 2012.
- Hersbach, H., Bell, B., Berrisford, P., Hirahara, S., Horányi, A., Muñoz-Sabater, J., Nicolas, J., Peubey, C., Radu, R., Schepers, D., Simmons, A., Soci, C., Abdalla, S., Abellan, X., Balsamo, G., Bechtold, P., Biavati, G., Bidlot, J., Bonavita, M., De Chiara, G., Dahlgren, P., Dee, D., Diamantakis, M., Dragani, R., Flemming, J., Forbes, R., Fuentes, M., Geer, A., Haimberger, L., Healy, S., Hogan, R. J., Hólm, E.,
500 Janisková, M., Keeley, S., Laloyaux, P., Lopez, P., Lupu, C., Radnoti, G., de Rosnay, P., Rozum, I., Vamborg, F., Villaume, S., and Thépaut, J.: The ERA5 global reanalysis, *Quarterly Journal of the Royal Meteorological Society*, 146, 1999–2049, <https://doi.org/10.1002/qj.3803>, 2020.
- Hua, D., Hao, X., Zhang, Y., and Qin, J.: Uncertainty assessment of potential evapotranspiration in arid areas, as estimated by the Penman-Monteith method, *Journal of Arid Land*, 12, 166–180, <https://doi.org/10.1007/s40333-020-0093-7>, 2020.
- 505 Jensen, M. E. and Haise, H. R.: Estimating Evapotranspiration from Solar Radiation, *Journal of the Irrigation and Drainage Division*, 89, 15–41, <https://doi.org/10.1061/JRCEA4.0000287>, 1963.
- Kuentz, A., Arheimer, B., Hundecha, Y., and Wagener, T.: Understanding hydrologic variability across Europe through catchment classification, *Hydrology and Earth System Sciences*, 21, 2863–2879, <https://doi.org/10.5194/hess-21-2863-2017>, 2017.
- Kumar, R., Samaniego, L., and Attinger, S.: Implications of distributed hydrologic model parameterization on water fluxes at multiple scales
510 and locations, *Water Resources Research*, 49, 360–379, <https://doi.org/10.1029/2012WR012195>, 2013.
- Kumar, R., Heße, F., Rao, P. S. C., Musolff, A., Jawitz, J. W., Sarrazin, F., Samaniego, L., Fleckenstein, J. H., Rakovec, O., Thober, S., and Attinger, S.: Strong hydroclimatic controls on vulnerability to subsurface nitrate contamination across Europe, *Nature Communications*, 11, 6302, <https://doi.org/10.1038/s41467-020-19955-8>, 2020.
- Liu, C., Wang, Z., Zheng, H., Zhang, L., and Wu, X.: Development of Hydro-Informatic Modelling System and its application, *Science in China Series E: Technological Sciences*, 51, 456–466, <https://doi.org/10.1007/s11431-008-0040-x>, 2008.
- Liu, Y., Jiang, Q., Wang, Q., Jin, Y., Yue, Q., Yu, J., Zheng, Y., Jiang, W., and Yao, X.: The divergence between potential and actual evapotranspiration: An insight from climate, water, and vegetation change, *Science of The Total Environment*, 807, 150648, <https://doi.org/10.1016/j.scitotenv.2021.150648>, 2022.
- Lu, J., Sun, G., McNulty, S. G., and Amatya, D. M.: A COMPARISON OF SIX POTENTIAL EVAPOTRANSPIRATION METHODS FOR
520 REGIONAL USE IN THE SOUTHEASTERN UNITED STATES, *Journal of the American Water Resources Association*, 41, 621–633, <https://doi.org/10.1111/j.1752-1688.2005.tb03759.x>, 2005.



- Massari, C., Avanzi, F., Bruno, G., Gabellani, S., Penna, D., and Camici, S.: Evaporation enhancement drives the European water-budget deficit during multi-year droughts, *Hydrology and Earth System Sciences*, 26, 1527–1543, <https://doi.org/10.5194/hess-26-1527-2022>, 2022.
- 525 Mazzoleni, M., Brandimarte, L., and Amaranto, A.: Evaluating precipitation datasets for large-scale distributed hydrological modelling, *Journal of Hydrology*, 578, 124 076, <https://doi.org/10.1016/j.jhydrol.2019.124076>, 2019.
- Maček, U., Bezak, N., and Šraj, M.: Reference evapotranspiration changes in Slovenia, *Europe, Agricultural and Forest Meteorology*, 260–261, 183–192, <https://doi.org/10.1016/j.agrformet.2018.06.014>, 2018.
- McGuinness, J. L. and Bordne, E. F.: A comparison of lysimeter-derived potential evapotranspiration with computed values, US Department of Agriculture, ISBN 0082-9811, issue: 1452, 1972.
- 530 Milly, P. C. D. and Dunne, K. A.: Potential evapotranspiration and continental drying, *Nature Climate Change*, 6, 946–949, <https://doi.org/10.1038/nclimate3046>, 2016.
- Muñoz-Sabater, J., Dutra, E., Agustí-Panareda, A., Albergel, C., Arduini, G., Balsamo, G., Boussetta, S., Choulga, M., Harrigan, S., Hersbach, H., Martens, B., Miralles, D. G., Piles, M., Rodríguez-Fernández, N. J., Zsoter, E., Buontempo, C., and Thépaut, J.-N.: ERA5-Land: a state-of-the-art global reanalysis dataset for land applications, *Earth System Science Data*, 13, 4349–4383, <https://doi.org/10.5194/essd-13-4349-2021>, 2021.
- Ndiaye, P. M., Bodian, A., Dezetter, A., Ogilvie, A., and Goudiaby, O.: Sensitivity of global hydrological models to potential evapotranspiration estimation methods in the Senegal River Basin (West Africa), *Journal of Hydrology: Regional Studies*, 53, 101 823, <https://doi.org/10.1016/j.ejrh.2024.101823>, 2024.
- 540 Oudin, L., Michel, C., and Anctil, F.: Which potential evapotranspiration input for a lumped rainfall-runoff model?, *Journal of Hydrology*, 303, 275–289, <https://doi.org/10.1016/j.jhydrol.2004.08.025>, 2005.
- Park, C.-E., Jeong, S.-J., Joshi, M., Osborn, T. J., Ho, C.-H., Piao, S., Chen, D., Liu, J., Yang, H., Park, H., Kim, B.-M., and Feng, S.: Keeping global warming within 1.5 °C constrains emergence of aridification, *Nature Climate Change*, 8, 70–74, <https://doi.org/10.1038/s41558-017-0034-4>, 2018.
- 545 Penman, H. L.: Natural evaporation from open water, bare soil and grass, *Proceedings of the Royal Society of London. Series A. Mathematical and Physical Sciences*, 193, 120–145, number: 1032 ISBN: 0080-4630 Publisher: The Royal Society London, 1948.
- Pfeifroth, U., Sanchez-Lorenzo, A., Manara, V., Trentmann, J., and Hollmann, R.: Trends and Variability of Surface Solar Radiation in Europe Based On Surface- and Satellite-Based Data Records, *Journal of Geophysical Research: Atmospheres*, 123, 1735–1754, <https://doi.org/10.1002/2017JD027418>, 2018.
- 550 Pimentel, R., Arheimer, B., Crochemore, L., Andersson, J. C. M., Pechlivanidis, I. G., and Gustafsson, D.: Which Potential Evapotranspiration Formula to Use in Hydrological Modeling World-Wide?, *Water Resources Research*, 59, e2022WR033 447, <https://doi.org/10.1029/2022WR033447>, 2023.
- Pohl, F., Rakovec, O., Rebmann, C., Hildebrandt, A., Boeing, F., Hermanns, F., Attinger, S., Samaniego, L., and Kumar, R.: Long-term daily hydrometeorological drought indices, soil moisture, and evapotranspiration for ICOS sites, *Scientific Data*, 10, 281, <https://doi.org/10.1038/s41597-023-02192-1>, 2023.
- 555 Priestley, C. H. B. and Taylor, R. J.: On the assessment of surface heat flux and evaporation using large-scale parameters, *Monthly weather review*, 100, 81–92, iSBN: 1520-0493, 1972.



- Rakovec, O., Kumar, R., Mai, J., Cuntz, M., Thober, S., Zink, M., Attinger, S., Schäfer, D., Schrön, M., and Samaniego, L.: Multi-scale and Multivariate Evaluation of Water Fluxes and States over European River Basins, *Journal of Hydrometeorology*, 17, 287–307, <https://doi.org/10.1175/JHM-D-15-0054.1>, 2016.
- Rakovec, O., Mizukami, N., Kumar, R., Newman, A. J., Thober, S., Wood, A. W., Clark, M. P., and Samaniego, L.: Diagnostic Evaluation of Large-Domain Hydrologic Models Calibrated Across the Contiguous United States, *Journal of Geophysical Research: Atmospheres*, 124, 13 991–14 007, <https://doi.org/10.1029/2019JD030767>, 2019.
- Reaver, N. G. F., Kaplan, D. A., Klammler, H., and Jawitz, J. W.: Theoretical and empirical evidence against the Budyko catchment trajectory conjecture, *Hydrology and Earth System Sciences*, 26, 1507–1525, <https://doi.org/10.5194/hess-26-1507-2022>, 2022.
- Samaniego, L., Kumar, R., and Attinger, S.: Multiscale parameter regionalization of a grid-based hydrologic model at the mesoscale, *Water Resources Research*, 46, <https://doi.org/10.1029/2008WR007327>, 2010.
- Samaniego, L., Thober, S., Wanders, N., Pan, M., Rakovec, O., Sheffield, J., Wood, E. F., Prudhomme, C., Rees, G., Houghton-Carr, H., Fry, M., Smith, K., Watts, G., Hisdal, H., Estrela, T., Buontempo, C., Marx, A., and Kumar, R.: Hydrological Forecasts and Projections for Improved Decision-Making in the Water Sector in Europe, *Bulletin of the American Meteorological Society*, 100, 2451–2472, <https://doi.org/10.1175/BAMS-D-17-0274.1>, 2019.
- Schulzweida, U.: CDO User Guide, <https://doi.org/10.5281/ZENODO.7112925>, publisher: Zenodo Version Number: 2.1.0, 2022.
- Seiller, G. and Ancil, F.: How do potential evapotranspiration formulas influence hydrological projections?, *Hydrological Sciences Journal*, 61, 2249–2266, <https://doi.org/10.1080/02626667.2015.1100302>, 2016.
- Sen, P. K.: Estimates of the Regression Coefficient Based on Kendall’s Tau, *Journal of the American Statistical Association*, 63, 1379–1389, <https://doi.org/10.1080/01621459.1968.10480934>, 1968.
- Shaw, S. B. and Riha, S. J.: Assessing temperature-based PET equations under a changing climate in temperate, deciduous forests, *Hydrological Processes*, 25, 1466–1478, <https://doi.org/10.1002/hyp.7913>, 2011.
- Shi, H., Luo, G., Hellwich, O., He, X., Kurban, A., De Maeyer, P., and Van de Voorde, T.: Global dryland aridity changes indicated by atmospheric, hydrological, and vegetation observations at meteorological stations, *Hydrology and Earth System Sciences*, 27, 4551–4562, <https://doi.org/10.5194/hess-27-4551-2023>, 2023a.
- Shi, L., Wang, B., Liu, D. L., Feng, P., Cleverly, J., Li, L., Zhang, G., and Yu, Q.: Performance of potential evapotranspiration models across different climatic stations in New South Wales, Australia, *Journal of Hydrology: Regional Studies*, 50, 101 573, <https://doi.org/10.1016/j.ejrh.2023.101573>, 2023b.
- Shrestha, P. K., Samaniego, L., Rakovec, O., Kumar, R., Mi, C., Rinke, K., and Thober, S.: Toward Improved Simulations of Disruptive Reservoirs in Global Hydrological Modeling, *Water Resources Research*, 60, e2023WR035 433, <https://doi.org/10.1029/2023WR035433>, 2024.
- Tang, G., Clark, M. P., and Papalexiou, S. M.: EM-Earth: The Ensemble Meteorological Dataset for Planet Earth, *Bulletin of the American Meteorological Society*, 103, E996–E1018, <https://doi.org/10.1175/BAMS-D-21-0106.1>, 2022.
- Teuling, A. J., de Badts, E. A. G., Jansen, F. A., Fuchs, R., Buitink, J., Hoek van Dijke, A. J., and Sterling, S. M.: Climate change, reforestation/afforestation, and urbanization impacts on evapotranspiration and streamflow in Europe, *Hydrology and Earth System Sciences*, 23, 3631–3652, <https://doi.org/10.5194/hess-23-3631-2019>, 2019.
- Thackeray, C. W., Hall, A., Norris, J., and Chen, D.: Constraining the increased frequency of global precipitation extremes under warming, *Nature Climate Change*, 12, 441–448, <https://doi.org/10.1038/s41558-022-01329-1>, 2022.



- 595 Thober, S., Cuntz, M., Kelbling, M., Kumar, R., Mai, J., and Samaniego, L.: The multiscale routing model mRM v1.0: simple river routing at resolutions from 1 to 50 km, *Geoscientific Model Development*, 12, 2501–2521, <https://doi.org/10.5194/gmd-12-2501-2019>, 2019.
- Thornthwaite, C. W.: An Approach toward a Rational Classification of Climate, *Geographical Review*, 38, 55, <https://doi.org/10.2307/210739>, 1948.
- Vicente-Serrano, S. M., Azorin-Molina, C., Sanchez-Lorenzo, A., Revuelto, J., López-Moreno, J. I., González-Hidalgo, J. C., Moran-Tejeda, E., and Espejo, F.: Reference evapotranspiration variability and trends in Spain, 1961–2011, *Global and Planetary Change*, 121, 26–40, <https://doi.org/10.1016/j.gloplacha.2014.06.005>, 2014.
- 600 Voisin, N., Wood, A. W., and Lettenmaier, D. P.: Evaluation of Precipitation Products for Global Hydrological Prediction, *Journal of Hydrometeorology*, 9, 388–407, <https://doi.org/10.1175/2007JHM938.1>, 2008.
- World Meteorological Organization (WMO): State of Global Water Resources 2022, Tech. rep., Geneva, Switzerland, <https://wmo.int/publication-series/state-of-global-water-resources-2022>, 2023.
- 605 Xiang, K., Li, Y., Horton, R., and Feng, H.: Similarity and difference of potential evapotranspiration and reference crop evapotranspiration – a review, *Agricultural Water Management*, 232, 106 043, <https://doi.org/10.1016/j.agwat.2020.106043>, 2020.
- Xu, C.-Y. and Singh, V. P.: Evaluation and generalization of radiation-based methods for calculating evaporation, *Hydrological Processes*, 14, 339–349, [https://doi.org/10.1002/\(SICI\)1099-1085\(20000215\)14:2<339::AID-HYP928>3.0.CO;2-O](https://doi.org/10.1002/(SICI)1099-1085(20000215)14:2<339::AID-HYP928>3.0.CO;2-O), 2000.
- 610 Yang, Y., Roderick, M. L., Zhang, S., McVicar, T. R., and Donohue, R. J.: Hydrologic implications of vegetation response to elevated CO₂ in climate projections, *Nature Climate Change*, 9, 44–48, <https://doi.org/10.1038/s41558-018-0361-0>, 2019.
- Zhang, D., Liu, X., Zhang, Q., Liang, K., and Liu, C.: Investigation of factors affecting intra-annual variability of evapotranspiration and streamflow under different climate conditions, *Journal of Hydrology*, 543, 759–769, <https://doi.org/10.1016/j.jhydrol.2016.10.047>, 2016.
- Zhao, L., Xia, J., Xu, C.-y., Wang, Z., Sobkowiak, L., and Long, C.: Evapotranspiration estimation methods in hydrological models, *Journal of Geographical Sciences*, 23, 359–369, <https://doi.org/10.1007/s11442-013-1015-9>, 2013.
- 615 Zhou, J., Li, Q., Ye, A., Xu, S., Yuan, Y., Xu, S., Zhang, D., Zhao, X., Zhu, Y., Zhao, Y., Xue, D., Dou, J., Liu, C., Shi, W., Wei, W., and Yang, X.: An improved methodology for quantifying the impact of human activities on hydrological drought change, *Journal of Hydrology: Regional Studies*, 50, 101 603, <https://doi.org/10.1016/j.ejrh.2023.101603>, 2023.